

The Involvement of the Mitochondrial Amidoxime Reducing Component (mARC) in the Reductive Metabolism of Hydroxamic Acids[□]

Carsten Ginsel, Birte Pnitzko, Danilo Froriep, Diana A. Stolfa, Manfred Jung, Christian Kubitzka, Axel J. Scheidig, Antje Havemeyer, and Bernd Clement

Pharmaceutical Institute, Department of Pharmaceutical and Medicinal Chemistry (C.G., B.P., D.F., A.H., B.C.) and Zoological Institute, Structural biology (C.K., A.J.S.), Christian-Albrechts-Universität zu Kiel, Kiel, Germany; and Institute of Pharmaceutical Sciences, Albert-Ludwig-Universität Freiburg, Freiburg, Germany (D.A.S., M.J.)

Received May 18, 2018; accepted July 11, 2018

ABSTRACT

The mitochondrial amidoxime reducing component is a recently discovered molybdenum enzyme in mammals which, in concert with the electron transport proteins cytochrome b5 and NADH cytochrome b5 reductase, catalyzes the reduction of *N*-oxygenated structures. This three component enzyme system plays a major role in *N*-reductive drug metabolism. Belonging to the group of *N*-hydroxylated structures, hydroxamic acids are also potential substrates of the mARC-system. Hydroxamic acids show a variety of pharmacological activities and are therefore often found in drug candidates. They can also exhibit toxic properties as is the case for many aryl hydroxamic acids formed during the metabolism of arylamides. Biotransformation assays using recombinant human proteins, subcellular porcine tissue fractions as well as human cell culture were performed. Here the mARC-dependent reduction of the

model compound benzhydroxamic acid is reported in addition to the reduction of three drugs. In comparison with other known substrates of the molybdenum depending enzyme system (e.g., amidoxime prodrugs) the conversion rates measured here are slower, thereby reflecting the mediocre metabolic stability and oral bioavailability of distinct hydroxamic acids. Moreover, the toxic *N*-hydroxylated metabolite of the analgesic phenacetin, *N*-hydroxyphenacetin, is not reduced by the mARC-system under the chosen conditions. This confirms the high toxicity of this component, as it needs to be detoxified by other pathways. This work highlights the need to monitor the *N*-reductive metabolism of new drug candidates by the mARC-system when evaluating the metabolic stability of hydroxamic acid-containing structures or the potential risks of toxic metabolites.

Introduction

Hydroxamic acids are a class of substances with a variety of biologic activities, including antibiotic (Barb et al., 2007; Halouska et al., 2014) and anti-inflammatory activities (Brogden et al., 1975), along with inhibitory properties toward metalloproteinases (Dalvie et al., 2008; Verma, 2012) and histone-deacetylases (HDACs) (Dokmanovic et al., 2007; Zhang and Zhong, 2014). The latter is of particular interest, as inhibitors of HDACs show antineoplastic activities and are currently applied in cancer treatment with new candidates under development (Wagner et al., 2010; Zhang and Zhong, 2014). Examples are vorinostat (suberoylanilide hydroxamic acid) which is marketed as Zolanza for the treatment of T-cell lymphoma and Panabinstat (Farydak) which has just been approved (Raedler, 2016).

D.A.S. and M.J. received funding from the European Union's Seventh Framework Program for research, technological development and demonstration under grant agreements nr. 241865 (SETReND).

<https://doi.org/10.1124/dmd.118.082453>.

□ This article has supplemental material available at dmd.aspetjournals.org.

Applying compounds with hydroxamic acids in therapy requires a reasonable level of metabolic stability. One expectable metabolic pathway, besides conjugation reactions, is hydrolysis to the corresponding carboxylic acid (Liu et al., 2014). As shown in Fig. 1, another likely metabolic conversion is the reduction of hydroxamic acids to the corresponding amide (Lowenthal, 1954; Hirsch and Kaplan, 1961; Kitamura and Tatsumi, 1985; Kiesel et al., 2013). For example, metabolism studies of CP544439, a hydroxamic acid-containing matrix metalloproteinase inhibitor, revealed the formation of the amide, the glucuronide and the carboxylic acid as the main metabolites of the orally administered drug (Dalvie et al., 2008). Besides their pharmacological advantages, aryl hydroxamic acids have been shown to possess toxic and mutagenic properties (Miller et al., 1961; Vaught et al., 1981). For example, the analgesic drug “Phenacetin” is *N*-hydroxylated during metabolism to yield *N*-hydroxyphenacetin (Hinson and Mitchell, 1976; Wirth et al., 1980). Phenacetin was withdrawn from the market because it was found to induce severe renal papillary necrosis and tumors of the renal pelvis and bladder in humans (Liu et al., 1972; Bengtsson et al., 1978). *N*-hydroxyphenacetin has been held responsible for these severe

ABBREVIATIONS: ACN, acetonitrile; BCA, bichinchoninic acid; bs, broad singlet; CI, chemical ionization; CYB5B, cytochrome b5 type B; CYB5R3, NADH-cytochrome b5 reductase 3; d, doublet; dd, double doublet; DMSO, dimethyl sulfoxide; DS116, *N*'-phenyloctanediamide; DS92, 8-oxo-8-(phenylamino)octanoic acid; dt, double triplet; EI, electron ionization; ESI, electrospray ionization; FBS, fetal bovine serum; HDACs, histone deacetylases; HPLC, high performance liquid chromatography; J, coupling constant in Hz; LOQ, limit of quantification; m, multiplet; mARC, mitochondrial amidoxime reducing component; mp, melting point; NMR, nuclear magnetic resonance; PCI, positive chemical ionization; rt, retention time; s, singlet; t, triplet; TLC, thin layer chromatography; UV, ultra violet; δ , chemical shift in ppm.

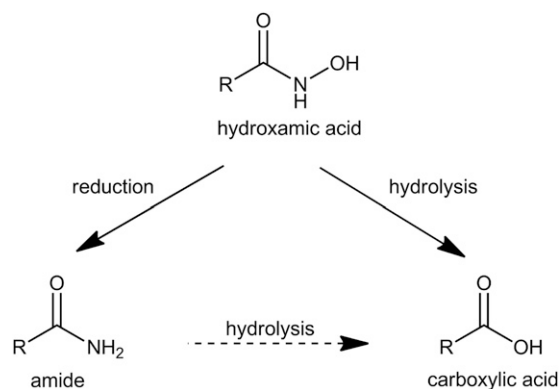


Fig. 1. Metabolism of hydroxamic acids. Hydroxamic acids can either undergo reduction to the corresponding amide or hydrolysis to the corresponding carboxylic acid. A hydrolysis of the amide to the carboxylic acid might be possible.

effects as it conducts similar pathways to many aromatic amines leading to the formation of DNA adducts (Vaught et al., 1981). In vivo and in vitro, *N*-hydroxyphenacetin is metabolized to Phenacetin (Fischbach and Lenk, 1985). The enzymatic basics of the reductive metabolism remain undetermined. The involvement of the cytochrome P450 isoform 2S1 in this reductive metabolism could be excluded (Wang and Guengerich, 2013).

It is well accepted that the mitochondrial amidoxime-reducing component “mARC”, together with the electron transport proteins cytochrome b5 and NADH-cytochrome b5 reductase, forms an *N*-reductive three component enzyme system located in the outer mitochondrial membrane which plays a major role in *N*-reductive drug metabolism. It has been shown after in vitro reconstitution and in cell culture that the mARC-system is responsible for the reduction of various *N*-hydroxylated compounds like amidoximes, *N*-hydroxyguanidines or sulfhydroxamic acids, hydroxylamines and *N*-oxides (Plitzko et al., 2013; Ott et al., 2015). Our laboratory has recently shown that mARC is a mitochondrial, molybdenum-containing enzyme (Havemeyer et al., 2006). All of the currently analyzed and completely annotated mammalian genomes code for two mARC proteins (mARC1 and mARC2) which share a high degree of sequence identity to each other (Wahl et al., 2010). Though the endogenous function of mARC is still not fully understood, mARC proteins are assumed to be involved in detoxification of mutagenic and toxic aromatic hydroxylamines like *N*-hydroxylated DNA-base analogs (Krompholz et al., 2012; Plitzko et al., 2015). The involvement in energy and NO metabolism has been discussed (Kotthaus et al., 2011; Neve et al., 2012; Jakobs et al., 2014; Sparacino-Watkins et al., 2014). In this study we examined whether the mARC-system is also capable of reducing hydroxamic acids and is thus involved in the metabolic conversion of this substance class. As shown in Fig. 2, we assayed the *N*-reduction of the model substrate benzhydroxamic acid and of four relevant pharmaceutical compounds (vorinostat, bufexamac and CP544439 as drugs and *N*-hydroxyphenacetin as a toxic drug metabolite) by performing biotransformation assays in the reconstituted recombinant human *N*-reductive system and in subcellular porcine liver fractions. Additionally, by performing metabolism studies and RNAi-mediated down-regulations of mARC in HEK-293 cells, the physiologic relevance of the *N*-reduction of hydroxamic acids in human cell metabolism was evaluated.

Materials and Methods

Reagents and Cell Lines

Unless otherwise stated all chemicals were purchased from Carl Roth GmbH & co. KG (Karlsruhe, Germany), Sigma Aldrich (St. Louis, MO) or Fluka (Buchs,

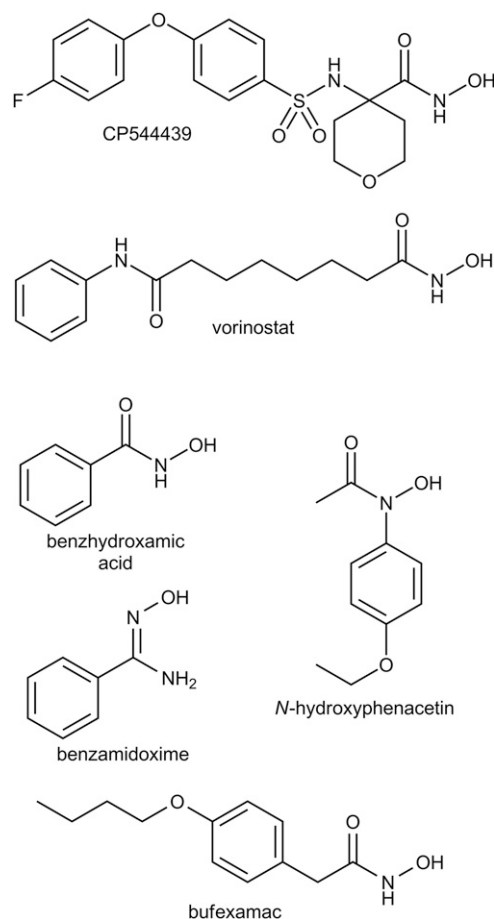


Fig. 2. Structures of all studied compounds.

Switzerland) and used without further purification. Methanol (HPLC grade) was from JT Baker (Deventer, Netherlands). Acetonitrile (HPLC grade) was from Honeywell (Seelze, Germany). Benzoic acid and chlorosulfonic acid were from Merck KGaA (Darmstadt, Germany). Ethyl 4-aminotetrahydro-2H-pyran-4-carboxylate hydrochloride and 4-fluorophenoxybenzene were from abcr (Karlsruhe, Germany). 4-nitrophenetole, 4-butoxyphenylacetic acid and sodium 1-octanesulfonate were from TCI (Zwijndrecht, Belgium). HEK-293 human embryonic kidney cells were purchased from Cell Lines Service (Eppelheim, Germany). Opti-MEM, minimum essential medium, sodium pyruvate solution, sodium bicarbonate, minimum Eagles’s medium nonessential amino acids, FBS, trypsin, L-glutamine, PBS, Lipofectamine RNAiMAX, Stealth Select RNAi siRNA targeting human MOSC1 (MOSC1HSS127704), and Stealth Select RNAi siRNA negative control were obtained from Invitrogen (Carlsbad, CA). ONTARGETplus SMARTpool siRNA targeting human MOSC2 was purchased from Thermo Scientific (Waltham, MA). Complete protease inhibitor cocktail was acquired from Roche Applied Science (Mannheim, Germany). Benzamidoxime was synthesized from benzonitrile and hydroxylamine (Krüger, 1885). For the synthesis of CP544439 (4-((4-(4-fluorophenoxy)phenyl)-sulfonylamino)-tetrahydropyran-4-carboxyhydroxamic acid) and its metabolites see Supplemental Data.

Synthesis of Vorinostat (Suberoanilohydroxamic Acid) and Metabolites

Chromatographic separations were performed on silica gel (15–40 mesh; Merck) using flash methodology. Reaction progress was monitored by analytical TLC on pre-coated silica gel (Kieselgel 60 F254) plates, and spots were detected by UV light (λ 254 nm). mp of the final target HDAC inhibitors were determined by the open capillary method on a Stuart-Scientific SMP3 electrothermal apparatus and are uncorrected. ^1H NMR spectra were recorded in the indicated deuterated solvents on a Bruker Avance DRX 400 MHz spectrometer and ^{13}C NMR on a Varian 100 MHz. Signals due to OH and NH protons were located by

deuterium exchange with D₂O. EI- and CI-mass spectra were measured with a TSQ700 mass spectrometer (ThermoFisher, Waltham, MA). ESI- and PCI-mass spectra were recorded with a LCQ-Advantage mass spectrometer. In all cases, spectroscopic data are in agreement with known compounds and assigned structures. HPLC purity determinations were performed on a JASCO HPLC system under isocratic conditions, using a Phenomenex Synergi Hydro RP-C18 column (250 × 4.6 mm, 4 μm particle size). Elution was performed using 0.05% of TFA in water/ACN 60/40 (v/v), at room temperature. The purity of all tested compounds was ≥98%, as measured by HPLC. Injection volumes were 2 μl, flow rate was 0.5 ml/min, detection was performed with UV (λ = 254 nm). All chromatographic and spectroscopic data were in accordance with literature data.

Synthesis of Vorinostat. Vorinostat was synthesized according to Mai et al. (2001). Retention time for HPLC was 7.8 minutes.

Synthesis of DS92. DS92 was synthesized by a modification of the procedure described in the literature (Suzuki et al., 2005). Suberic acid (5.00 g, 28.7 mmol) was slowly added to neat freshly distilled aniline (2.70 ml, 30.1 mmol) and the mixture was stirred at 185°C and left at the same temperature for 2 hour. The mixture was cooled to room temperature and a NaOH 2 N aqueous solution was added to set the pH of the mixture at ~8. The suspension was filtered and the filtrate was acidified to pH~2, obtaining a white precipitate that was collected and suspended in warm water (50°C). The insoluble part was filtered and washed with hot water, yielding DS92 as white pure precipitate (3.93 g, 55%). R_f = 0.35 (EtOAc/Cy, 8:2); Retention time for HPLC was 14.5 minute; mp = 124–126°C; ¹H-NMR (400 MHz, d₆DMSO): δ 1.23–1.35 (m, 4H), 1.42–1.52 (m, 2H), 1.54–1.63 (m, 2H), 2.20 (t, J = 7.4 Hz, 2H), 2.29 (t, J = 7.4 Hz, 2H), 7.01 (tt, J = 7.6; J = 1.1 Hz, 1H), 7.28 (t, J = 7.6 Hz, 2H), 7.58 (dd, J = 8.7; J = 1.1 Hz, 2H), 9.85 (s, 1H), 11.97 (br s, 1H); LRMS (ESI) m/z 248.1 [M-H]⁻.

Synthesis of DS116. DS116 was obtained by a fast two-step synthesis starting from the carboxylic acid derivative DS92, which is transformed using thionyl chloride into the corresponding acyl chloride, further reacted into the target according to an already described procedure (Wright and Corbett, 1993). To a solution of 8-oxo-8-(phenylamino)octanoic acid (0.30 g, 1.2 mmol) in dry DCM (3 ml) thionyl chloride (330 μl, 4.6 mmol) was slowly added at room temperature. The solution was heated to reflux for 3 hour and later a stream of nitrogen was used to remove the solvent and the excess of thionyl chloride. To the crude product was added a solution of concentrated aqueous ammonia solution (1.03 ml, 26.4 mmol) and NH₄Cl (0.22 g, 4.1 mmol) in 1 ml of water and the mixture was stirred at 20°C for 8 hour. The reaction was quenched with NaBH₄ (23 mg, 0.6 mmol) and after 1 hour at room temperature HCl 2 N aqueous solution was added dropwise to pH~2. The precipitate was collected to give DS116 as white powder (0.24 g, 80%). R_f = 0.30 (DCM/Et₂O/MeOH, 9.5:1:0.5); Retention time for HPLC was 9.18 minute; mp = 161–163°C; ¹H-NMR (400 MHz, DMSO-d₆): δ 1.22–1.34 (m, 4H), 1.44–1.52 (m, 2H), 1.63–1.53 (m, 2H), 2.03 (t, J = 7.4 Hz, 2H), 2.29 (t, J = 7.4 Hz, 2H), 6.68 (br s, 1H), 7.01 (t, J = 7.4, 1H), 7.22 (br s, 1H), 7.28 (t, J = 7.8 Hz, 2H), 7.58 (d, J = 7.8 Hz, 2H), 9.85 (s, 1H); LRMS (ESI) m/z 247.1 [M-H]⁻.

Synthesis of *N*-Hydroxyphenacetin

N-hydroxyphenacetin was prepared using a previously reported procedure with minor modifications (Hinson and Mitchell, 1976). 4-Nitrophenetole (2.0 g, 11.96 mmol) and NH₄Cl (0.64 g, 11.96 mmol) were dissolved in 40 ml of a C₂H₅OH/H₂O mixture (4:1, v/v) at room temperature. After the addition of Zn dust (3.2 g, 48.94 mmol) the reaction mixture was stirred for 10 minutes. The Zn dust was filtered and washed with 40 ml (C₂H₅)₂O. The ethereal phase was washed with 50 ml brine and separated from the aqueous phase. NaHCO₃ (1.6 g, 19.04 mmol) was suspended in 5 ml H₂O at 0°C and the *N*-hydroxyphenetidine containing ethereal phase was added. 500 μl of 2.5% acetyl chloride in (C₂H₅)₂O were slowly added over 1 hour. The formation of the product was TLC controlled. *N*-hydroxyphenacetin gave a red, *N*-hydroxyphenetidine a blue spot with FeCl₃. After disappearance of the blue spot, 20 ml of H₂O was added and twice extracted with (C₂H₅)₂O. The combined layers were washed with H₂O and twice with brine. The product was extracted with 100 ml of cold 0.2 M NH₃-solution. After neutralization to pH 7.0 with NaHCO₃ the product was extracted in 300 ml (C₂H₅)₂O, dried over anhydrous Na₂SO₄ and the solvent was evaporated to dryness. *N*-hydroxyphenacetin was recrystallized with (C₂H₅)₂O/hexane, 15% yield from 4-nitrophenetole. ¹H-NMR (300 MHz, DMSO-d₆): δ 10.48 (s, 1H, hydroxyl), 7.45 (d, J = 8.7 Hz, aromatic, 2H), 6.91 (d, J = 9.1 Hz, aromatic, 2H), 4.01 (q, J = 7.0 Hz, 2H, H₃CH₂-), 2.14 (s, 3H, CH₃CO⁻), 1.31 (t, J = 7.0 Hz, 3H, CH₃CH₂-); LC-MS (ESI), m/z 196 [M+H]⁺, 178, 150.

Protein Sources

Subcellular porcine tissue fractions were purified from female pigs as described earlier (Ott et al., 2014). Expression and purification of human mARC1 (reference sequence NP_073583) and mARC2 (reference sequence NP_060368), CYB5B (reference sequence NP_085056) and CYB5R3 (reference sequence NP_000389) was carried out in *Escherichia coli* as described by Wahl et al. (2010). Protein content was determined using (BCA) protein assay kit (Pierce, Rockford, IL) according to the manufacturer's protocol. Heme content in CYB5B was determined according to the method of Estabrook by recording the difference spectrum of oxidized and NADH-reduced protein (Estabrook and Werringloer, 1978). FAD-content in CYB5R3 was measured at 450 nm according to Whitby after sample preparation by heating at 100°C for 10 minute and centrifugation at 22,000g for 5 minute at room temperature (Whitby, 1953). For the quantification of FAD a calibration curve (0.01–0.1 mM) was used.

In Vitro *N*-Reductive Activity Assay

In vitro biotransformation assay was carried out at 37°C in a shaking water bath. Incubation mixture consisted of 100 μg of porcine subcellular fractions in 100 mM potassium phosphate buffer, pH 6.0 or in case of recombinantly expressed human proteins of 7.5 μg mARC1 or mARC2, CYB5B resulting in 75 pmol heme and CYB5R3 resulting in 7.5 pmol FAD in 20 mM MES buffer, pH 6.0. Different substrate concentrations were used and for CP544439, vorinostat and bufexamac 4.0%, 4.8% and 8.0% DMSO were added respectively. After 3 minute of pre-incubation, the reaction was started by adding 1 mM NADH, resulting in a total volume of 150 μl. Incubation was stopped after 15 minute by adding 150 μl of cold methanol. Afterward, samples were shaken for 5 minute at room temperature and centrifuged for 5 minute with 9500g at room temperature. Supernatants were analyzed by HPLC. For the determination of kinetic parameters with recombinantly expressed human protein the DMSO concentration was kept at the same level and only the substrate concentration was modified.

HPLC Analysis for Incubated Samples

The flow rate was kept at 1.0 ml/min and the injection volume was 10 μl for all performed HPLC analysis. All benzhydroxamic acid and CP544439 related samples were measured on a Waters e2695 Separation Module with a Waters 2998 Photodiode Array Detector and Waters Empower 2 Build 2154 as integration software.

For the separation of benzhydroxamic acid (rt = 5.0 ± 0.2 minute) benzamide (rt = 8.1 ± 0.2 minute) and benzoic acid (rt = 12.7 ± 0.1 minute) a Phenomenex Gemini NX-C18 (5 μm), 150 × 4.6 mm with a Phenomenex C18 4 × 3.0 mm pre-column was used. The mobile phase consisted of 50 mM KH₂PO₄, pH 4.6, 10 mM tetramethylammonium chloride and 10% acetonitrile (v/v). Detection wavelength was 210 nm.

For the separation of CP544439 (rt = 4.8 ± 0.3 minute), deoxy CP544439 (rt = 5.9 ± 0.2 minute) and the carboxylic derivative (rt = 7.0 ± 0.2 minute) a Waters Sunfire C18, 3.5 μm, 150 × 4.6 mm with a Phenomenex C18 4 × 3.0 mm pre-column was used. Solvent A (0.2% formic acid in H₂O (v/v)) and Solvent B (0.2% formic acid in acetonitrile (v/v)) were used. Starting with 60% A, the gradient changed linearly from 3 to 7 minute to 10% A. At 11 minute A was set to 60% over 0.5 minute. Total runtime was 16 minute. Detection wavelength was 247 nm. The column temperature was maintained at 25°C and sample storage temperature at 18°C.

All vorinostat, bufexamac, *N*-hydroxyphenacetin and benzamidoxime related samples were measured on a Waters HPLC system consisting of a Waters 717 autosampler, a Waters 1525 pump and a Waters 2487 dual absorbance detector at room temperature. A Phenomenex Gemini NX-C18 (5 μm), 150 × 4.6 mm with a Phenomenex C18 4 × 3.0 mm pre-column was used with exception for benzamidoxime where a LiChrospher 60 RP-select B (5 μm), 250 × 4 mm column combined with a LiChrospher 60 RP-select pre-column was used.

For separation of vorinostat (rt = 6.7 ± 0.0 minute), DS116 (rt = 8.9 ± 0.1 minute) and DS92 (rt = 18.9 ± 0.2 minute) the mobile phase consisted of 100 mM KH₂PO₄ and 23% acetonitrile (v/v). The detection wavelength was set to 254 nm.

For separation of bufexamac (rt = 16.9 ± 0.1 minute), deoxy bufexamac (rt = 20.9 ± 0.1 minute) and the carboxylic derivative (rt = 28.5 ± 0.2 minute) the mobile phase consisted of 50 mM KH₂PO₄, pH 4.4, 10 mM tetramethylammonium chloride and 45% methanol (v/v). Detection wavelength was set to 228 nm.

For separation of *N*-hydroxyphenacetin ($rt = 7.8 \pm 0.2$ minute) and phenacetin ($rt = 9.1 \pm 0.0$ minute) the mobile phase consisted of 1% formic acid in H₂O (v/v) and 22.5% acetonitrile (v/v). Detection wavelength was 245 nm.

For separation of benzamidoxime ($rt = 9.1 \pm 0.3$ minute) and benzamidine ($rt = 15.9 \pm 0.1$ minute) the mobile phase consisted of 10 mM sodium 1-octanesulfonate and 20% acetonitrile. Detection wavelength was 229 nm.

Cell Culture

HEK-293 cells, derived from a female human source, were maintained in minimum essential medium supplemented with 10% FBS, 2 mM L-glutamine, 0.1 mM nonessential amino acids, 1 mM sodium pyruvate, and 1.5 g/l sodium bicarbonate. The cell line was incubated at 37°C in 5% CO₂.

siRNA Transfection and Design of Knockdown Experiments

HEK-293 cells were reverse transfected and mARC-protein down-regulated according to the previous described procedure (Plitzko et al., 2015).

N-Reductive Metabolism of Benzhydroxamic Acid in HEK 293 Cells

For *N*-reduction studies in HEK-293 the culture medium was removed, and cells were carefully washed and pre-incubated with substrate-free incubation buffer (Hanks' balanced salt solution containing 10 mM HEPES, pH 7.4) at 37°C for 10 minute. After removing the substrate-free incubation buffer, the vital cells were then incubated with benzhydroxamic acid-containing incubation buffer (3 mM, 0.5% (v/v) DMSO) at 37°C for 180 minute. After the designated time, the culture supernatant was carefully removed, centrifuged to eliminate cellular debris and analyzed by HPLC as described above.

Total Cellular Protein Extraction

Cellular protein was harvested and protein contents determined as previously described (Plitzko et al., 2015).

Western Blot Analysis

SDS-PAGE and Western Blot analysis to verify down-regulation of mARC-protein in HEK-293 cells was carried out as described previously (Plitzko et al., 2015).

Statistical Analysis

Statistical analyses were carried out using the SigmaPlot 11 software (Systat Software Inc., Erkrath, Germany). The significance of observed differences was evaluated by Bonferroni test. A probability less than 5% was considered to be significant. All experimental values are given as means \pm S.D.

Results

From all analyzed subcellular fractions, *N*-reductive activity in mitochondria was found to be enhanced compared with other tissue fractions for all *N*-unsubstituted hydroxamic acids (Fig. 3). These findings reflect the enrichment of mARC depending enzyme activities in this fraction as published earlier (Krompholz et al., 2012). In the microsomal and cytosolic fractions only minor/no *N*-reductive activity was detectable. By contrast, no reduction of *N*-hydroxyphenacetin could be detected after incubation with the

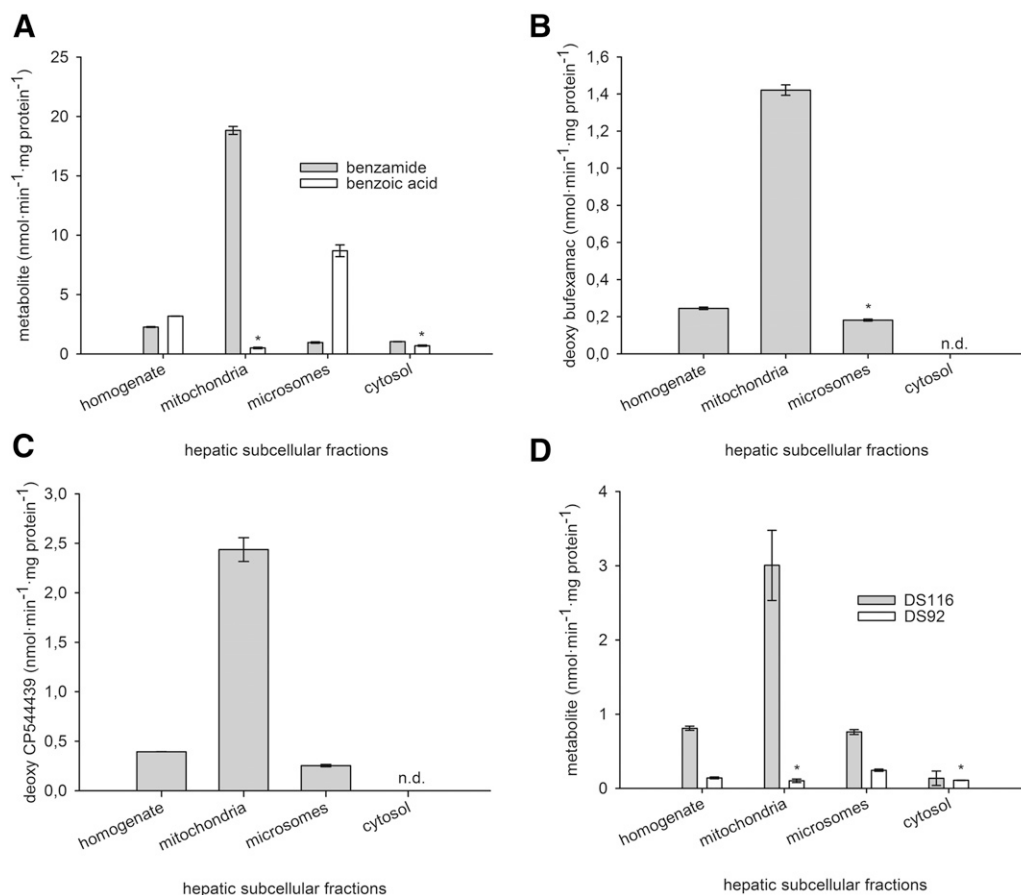


Fig. 3. *N*-reduction of benzhydroxamic acid, bufexamac, CP544439 and vorinostat in hepatic subcellular fractions. Biotransformation assay consisted of 100 μ g protein, 1 mM NADH and either 1.0 mM vorinostat and 4.8% DMSO, 3.0 mM benzhydroxamic acid, 0.5 mM CP544439 and 4.0% DMSO or 1.0 mM bufexamac and 8.0% DMSO. Incubation was carried out for 15 minute and stopped by addition of methanol. Activities are means \pm S.D. of two biologic determinations. (A) benzhydroxamic acid, (B) bufexamac, (C) CP544439, (D) vorinostat, *under limit of quantification, n.d. not detectable.

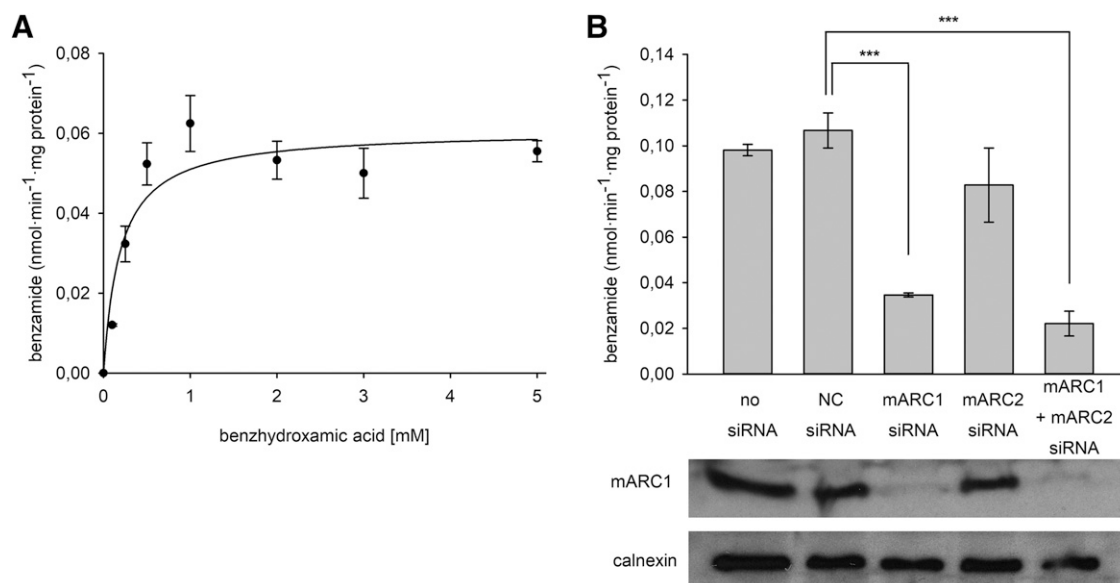


Fig. 4. *N*-reductive metabolism of benzhydroxamic acid in HEK-293 cells. *N*-reductive activities of cells were determined as described in *Materials and Methods*. Results are presented as means \pm S.D. ($n = 3$). (A) Substrate dependent metabolism. Incubation time was 180 minute. (B) Effect of mARC knockdown on *N*-reduction. HEK-293 cells were transfected with 20 nM mARC siRNA or non-targeting (NC) siRNA. The siRNA-mediated down-regulations of the proteins of interest were verified by western blot using anti-mARC1, anti-mARC2 or anti-calnexin antibody. Calnexin levels were used as loading control. mARC2-protein could not be detected. *N*-reductive activities were determined on day 4 after transfection. *** $P < 0.001$.

mitochondrial fraction and only minor reduction rates were detected within the cytosolic fraction (data not shown). Besides reduction to the amide, hydrolysis to the corresponding carboxylic acids was monitored and was found to be more pronounced in microsomes compared with other fractions; this indicates the involvement of a microsomal enzymatic system or a non-enzymatic reaction (Fig. 3, A and D). In the case of bufexamac and CP544439 the microsomal fraction was the only fraction where hydrolysis could be detected to a small extent (data not shown).

To prove the involvement of mARC in the reduction of hydroxamic acids, a cell based siRNA experiment was performed. In HEK-293 cells reductive conversion of benzhydroxamic acid to benzamide occurs in a time-dependent (data not shown) and substrate-dependent manner (Fig. 4A) and followed Michaelis-Menten kinetics ($v_{\max} = 0.06 \pm 0.01$ nmol benzamide·min⁻¹·mg protein⁻¹). By siRNA-mediated down-regulation of mARC1, benzamide formation decreased dramatically to approximately 30% compared with the negative control (Fig. 4B). Knockdown of mARC2 in HEK-293 cells did not affect the reduction of benzhydroxamic acid in HEK-293 cells. This same behavior is also observed with the model substrate benzamidoxime and is attributed to the low level of mARC2-protein expression in HEK-293 cells (Plitzko et al., 2013). Simultaneous knockdown of both mARC-proteins led to a small, further decrease in *N*-reductive activity than was observed in the mARC1-only knockout experiments. To further elucidate the differences between mARC1 and mARC2 the kinetic parameters v_{\max} and K_M were determined with the in vitro reconstituted recombinant *N*-reductive system (Fig. 5). All hydroxamic acids were clearly reduced to the corresponding amides with the exception of *N*-hydroxyphenacetin. These results are consistent with previous observations in subcellular fractions. Benzhydroxamic acid, bufexamac, CP544439 and vorinostat were exclusively reduced to their corresponding amides; none of the corresponding carboxylic acid products were detected. The reductions obey Michaelis-Menten kinetics for both mARC-proteins. The calculated K_M and v_{\max} values are presented in Table 1. The conversion rates of

hydroxamic acids are lower in comparison with the model compound benzamidoxime (e.g., for vorinostat, v_{\max} is 15 times slower). For both incubation types with subcellular fractions and recombinant expressed proteins, highest v_{\max} values were obtained for the model compound benzhydroxamic acid in comparison with all other studied hydroxamic acids.

According to the v_{\max} values, CP544439 and vorinostat are reduced to the same amount and smallest conversion rates were detected for bufexamac. Vorinostat, bufexamac and CP544439 required the use of DMSO as a solubilizer. Due to the negative influence of high DMSO concentrations in the incubation mixture (see Supplemental Data), only the minimum amount of DMSO required for solubility was added. In the case of benzhydroxamic acid v_{\max} was about four times higher with mARC2 than with mARC1 but the K_M increased sevenfold. Only slight differences of the kinetic parameters for vorinostat and bufexamac were detected for both mARC forms, whereas CP544439 was exclusively reduced by mARC1. In accordance with the results obtained with subcellular liver fractions and RNAi studies all *N*-unsubstituted hydroxamic acids are reduced by mARC.

Discussion

The mARC-containing three component enzyme system is responsible for the reduction of various *N*-hydroxylated compounds (Ott et al., 2015) and the results of our recent investigations demonstrate clearly that hydroxamic acids belong to this class of compounds. The hydroxamate moiety exhibits strong cation chelating properties and thereby possesses the ability to affect a variety of enzymes. Hydroxamic acid moieties are found in a multitude of drugs and drug candidates (Halouska et al., 2014; Zhang and Zhong, 2014). In addition, aryl hydroxamic acids have been shown to possess toxic and mutagenic properties (Miller et al., 1961; Vaught et al., 1981). Therefore, the investigation of the metabolic fate of hydroxamic acids is of particular relevance for further drug developments and for the understanding of detoxification pathways. We could demonstrate that hydroxamic acids can serve as substrates for the mARC-system.

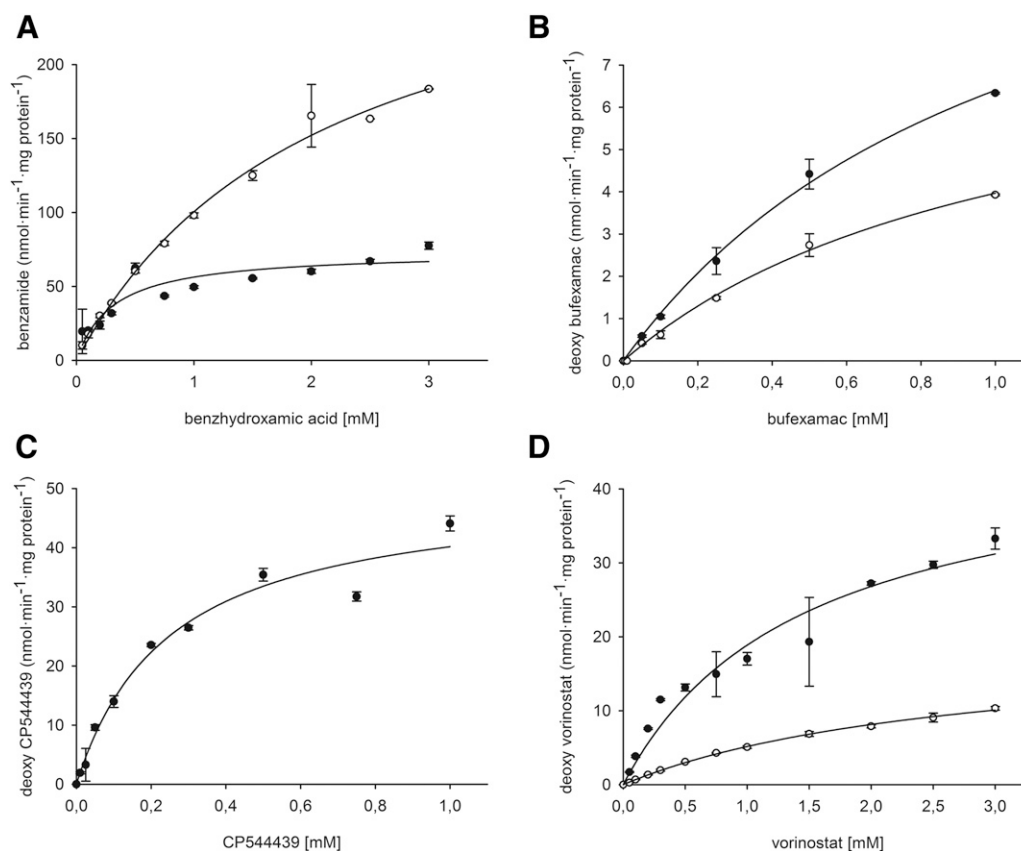


Fig. 5. Substrate concentration dependence for mARC1 (black) and mARC2 (white). Biotransformation assay consisted of 7.5 μg hmARC, 75 pmol CYB5B and 7.5 pmol CYB5R3. Incubation time was 15 minutes. Quantification was done by HPLC analysis. Activities are means \pm S.D. of two biologic determinations. (A) benzhydroxamic acid, (B) bufexamac, (C) CP544439, (D) vorinostat.

The model compound benzhydroxamic acid, as well as three other drugs (vorinostat, bufexamac and CP544439) are reduced to the corresponding amides by porcine mitochondria and the reconstituted recombinant human mARC-system (Table 1). The *N*-reduction observed *in vitro* is also evident in intact human cell metabolism and is mARC-dependent as the siRNA-mediated down-regulation leads to a dramatic decrease in *N*-reductive activity (Fig. 4B). HEK-293 cells were chosen because of the high *N*-reductive activity in renal tissue (Krompholz et al., 2012). However, the *N*-reductive conversion of hydroxamic acids is lower compared with the model compound (benzamidoxime). Amidoximes, used as pro-drugs for amidines, are rapidly reduced *in vivo* (Clement et al., 1992). In the case of hydroxamic acids, reduction leads to inactivation because the amide is not able to form strongly chelating complexes. As metabolism studies for CP544439 reveal, the main metabolism pathways of hydroxamic acids *in vivo* are glucuronidation, reduction and hydrolysis (Dalvie et al., 2008). The reduction to the amide is of great physiologic relevance, especially in rats, where the amide is the most prevalent metabolite. It has been demonstrated that the aldehyde oxidase is capable of reducing hydroxamic acids to amides (Sugihara et al., 1983a,b; Sugihara and Tatsumi, 1986). Reduction of CP544439 was proposed to be catalyzed by this enzyme as well; studies with human cytosolic liver fractions using the artificial electron donor *N*-methylnicotinamide resulted in a very low conversion rate (1.6 pmol·min⁻¹·mg protein⁻¹) (Obach, 2004). The aldehyde oxidase is located in the cytosol, but we could not detect any *N*-reductive activity in the porcine liver cytosol under our tested conditions (Fig. 5C). Our determined conversion rate with the

mitochondrial fraction for CP544439 is about 2.5 nmol·min⁻¹·mg protein⁻¹, which is more than 1500 times higher than the previous described cytosolic conversion rate. This finding indicates the important role of mARC in the reduction of hydroxamic acids to the amides. Interestingly, vorinostat has sufficient metabolic stability for therapy and is applied orally, but high doses of 400 mg/day are necessary (Mann et al., 2007). The enhanced lipophilicity of

TABLE 1

N-reduction of vorinostat, benzhydroxamic acid, bufexamac, CP544439, *N*-hydroxyphenacetin and benzamidoxime by the reconstituted recombinant mARC-system. Biotransformation assays were carried out as described in *Materials and Methods*

Activities are means \pm S.D. of two biologic determinations.

Substrate		K_m (mM)	v_{max} (nmol·min ⁻¹ ·mg protein ⁻¹)
vorinostat	mARC1	1.45 \pm 0.37	46.3 \pm 5.5
	mARC2	2.73 \pm 0.18	19.3 \pm 0.8
benzhydroxamic acid	mARC1	0.31 \pm 0.11	73.7 \pm 7.0
	mARC2	2.12 \pm 0.28	313.5 \pm 22.5
bufexamac	mARC1	1.09 \pm 0.15	13.4 \pm 1.1
	mARC2	1.07 \pm 0.15	8.2 \pm 0.7
CP544439	mARC1	0.25 \pm 0.06	50.2 \pm 4.4
	mARC2	—/—	—/— ^a
<i>N</i> -hydroxyphenacetin	mARC1	—/—	—/— ^b
	mARC2	—/—	—/— ^b
benzamidoxime	mARC1	0.63 \pm 0.06	674.8 \pm 25.1
	mARC2	0.54 \pm 0.03	549.6 \pm 12.1

^aLOQ = 0.9 nmol·min⁻¹·mg protein⁻¹.

^bLOQ = 3.5 nmol·min⁻¹·mg protein⁻¹.

vorinostat compared with benzhydroxamic acid and benzamidoxime could be a pivotal characteristic. The low conversion rates determined for bufexamac, which is a very lipophilic ether compound, support this theory (Fig. 5B). Studies to further elucidate structure activity relationships should be done to evaluate whether lipophilicity is an important feature for enzymatic conversion of hydroxamic acids by the mARC-system and to detect candidates with better stability toward *N*-reduction.

In the case of *N*-hydroxyphenacetin no reduction to the amide by mARC was observed. This is the first investigated hydroxamic acid studied by us so far which is not reduced. However, this could be an explanation for the high toxicity of this compound as it needs to be detoxified by other pathways. The most apparent difference between *N*-hydroxyphenacetin and the other studied hydroxamic acids is the substitution of the nitrogen's hydrogen with the sterically demanding phenyl group. Due to this steric hindrance mARC might not be able to bind and reduce such kind of substrates. This hypothesis needs to be proved by further structure activity studies.

In conclusion, to properly evaluate the metabolic stability of new hydroxamic acid containing drug candidates, metabolism by the mitochondrial mARC-system must be considered.

Acknowledgments

Thanks to Timothy Zerk for proofreading the article.

Authorship Contributions

Participated in research design: Scheidig, Havemeyer, Clement.

Conducted experiments: Ginsel, Plitzko.

Contributed new reagents or analytical tools: Ginsel, Froriep, Stofa, Jung.

Expression and purification of recombinant proteins: Kubitzka.

Performed data analysis: Ginsel, Plitzko.

Wrote or contributed to the writing of the manuscript: Ginsel, Plitzko, Clement.

References

Barb AW, McClerren AL, Snehelatha K, Reynolds CM, Zhou P, and Raetz CRH (2007) Inhibition of lipid A biosynthesis as the primary mechanism of CHIR-090 antibiotic activity in *Escherichia coli*. *Biochemistry* **46**:3793–3802.

Bengtsson U, Johansson S, and Angervall L (1978) Malignancies of the urinary tract and their relation to analgesic abuse. *Kidney Int* **13**:107–113.

Brogden RN, Pinder RM, Sawyer PR, Speight TM, and Avery GS (1975) Bufexamac: a review of its pharmacological properties and therapeutic efficacy in inflammatory dermatoses. *Drugs* **10**: 351–356.

Clement B, Immel M, Terlinden R, and Wingen F-J (1992) Reduction of amidoxime derivatives to pentamidine in vivo. *Arch Pharm (Weinheim)* **325**:61–62.

Dalvie D, Cosker T, Boyden T, Zhou S, Schroeder C, and Potchoiba MJ (2008) Metabolism distribution and excretion of a matrix metalloproteinase-13 inhibitor, 4-[4-(4-fluorophenoxy)-benzenesulfonylamino]tetrahydropyran-4-carboxylic acid hydroxyamide (CP-544439), in rats and dogs: assessment of the metabolic profile of CP-544439 in plasma and urine of humans. *Drug Metab Dispos* **36**:1869–1883.

Dokmanovic M, Clarke C, and Marks PA (2007) Histone deacetylase inhibitors: overview and perspectives. *Mol Cancer Res* **5**:981–989.

Estabrook RW and Werringer J (1978) The measurement of difference spectra: application to the cytochromes of microsomes. *Methods Enzymol* **52**:212–220.

Fischbach T and Lenk W (1985) The metabolism of *N*-hydroxyphenacetin in vitro and in vivo. *Xenobiotica* **15**:915–927.

Halouska S, Fenton RJ, Zinniel DK, Marshall DD, Barletta RG, and Powers R (2014) Metabolomics analysis identifies d-Alanine-d-Alanine ligase as the primary lethal target of d-Cycloserine in mycobacteria. *J Proteome Res* **13**:1065–1076.

Havemeyer A, Bittner F, Wollers S, Mendel R, Kunze T, and Clement B (2006) Identification of the missing component in the mitochondrial benzamidoxime prodrug-converting system as a novel molybdenum enzyme. *J Biol Chem* **281**:34796–34802.

Hinson JA and Mitchell JR (1976) *N*-Hydroxylation of phenacetin by hamster liver microsomes. *Drug Metab Dispos* **4**:430–435.

Hirsch PF and Kaplan NO (1961) The conversion of pyridine hydroxamic acids to amides by mouse liver mitochondria. *J Biol Chem* **236**:926–930.

Jakobs HH, Mikula M, Havemeyer A, Strzalkowska A, Borowa-Chmielak M, Dzwonek A, Gajewska M, Hennig EE, Ostrowski J, and Clement B (2014) The *N*-reductive system composed of mitochondrial amidoxime reducing component (mARC), cytochrome b5 (CYB5B) and cytochrome b5 reductase (CYB5R) is regulated by fasting and high fat diet in mice. *PLoS One* **9**: e105371.

Kiesel BF, Parise RA, Tjørnelund J, Christensen MK, Loza E, Tawbi H, Chu E, Kumar S, and Beumer JH (2013) LC-MS/MS assay for the quantitation of the HDAC inhibitor belinostat and five major metabolites in human plasma. *J Pharm Biomed Anal* **81–82**:89–98.

Kitamura S and Tatsumi K (1985) Purification of *N*-hydroxy-2-acetylaminofluorene reductase from rabbit liver cytosol. *Biochem Biophys Res Commun* **133**:67–74.

Kotthaus J, Wahl B, Havemeyer A, Kotthaus J, Schade D, Garbe-Schönberg D, Mendel R, Bittner F, and Clement B (2011) Reduction of *N*(ω)-hydroxy-L-arginine by the mitochondrial amidoxime reducing component (mARC). *Biochem J* **433**:383–391.

Krompholz N, Krischkowski C, Reichmann D, Garbe-Schönberg D, Mendel R-R, Bittner F, Clement B, and Havemeyer A (2012) The mitochondrial Amidoxime Reducing Component (mARC) is involved in detoxification of *N*-hydroxylated base analogues. *Chem Res Toxicol* **25**: 2443–2450.

Krüger P (1885) Ueber Abkömmlinge des Benzenylamidoxims. *Ber Dtsch Chem Ges* **18**: 1053–1060.

Liu L, Detering J-C, Milde T, Haefeli WE, Witt O, and Burhenne J (2014) Quantification of vorinostat and its main metabolites in plasma and intracellular vorinostat in PBMCs by liquid chromatography coupled to tandem mass spectrometry and its relation to histone deacetylase activity in human blood. *J Chromatogr B Analyt Technol Biomed Life Sci* **964**:212–221.

Liu T, Smith GW, and Rankin JT (1972) Renal pelvic tumour associated with analgesic abuse. *Can Med Assoc J* **107**:768, *passim*.

Lowenthal J (1954) Enzymatic conversion of salicylhydroxamic acid to salicylamide. *Nature* **174**: 36–37.

Mai A, Esposito M, Sbardella G, and Massa S (2001) A new facile and expeditious synthesis of *N*-hydroxy-*N'*-phenyloctanediamide, a potent inducer of terminal cytodifferentiation. *Org Prep Proced Int* **33**:391–394.

Mann BS, Johnson JR, Cohen MH, Justice R, and Pazdur R (2007) FDA approval summary: vorinostat for treatment of advanced primary cutaneous T-cell lymphoma. *Oncologist* **12**: 1247–1252.

Miller EC, Miller JA, and Hartmann HA (1961) *N*-Hydroxy-2-acetylaminofluorene: a metabolite of 2-acetylaminofluorene with increased carcinogenic activity in the rat. *Cancer Res* **21**:815–824.

Neve EPA, Nordling A, Andersson TB, Hellman U, Diczfalussy U, Johansson I, and Ingelman-Sundberg M (2012) Amidoxime reductase system containing cytochrome b5 type B (CYB5B) and MOSC2 is of importance for lipid synthesis in adipocyte mitochondria. *J Biol Chem* **287**: 6307–6317.

Obach RS (2004) Potent inhibition of human liver aldehyde oxidase by raloxifene. *Drug Metab Dispos* **32**:89–97.

Ott G, Havemeyer A, and Clement B (2015) The mammalian molybdenum enzymes of mARC. *J Biol Inorg Chem* **20**:265–275.

Ott G, Plitzko B, Krischkowski C, Reichmann D, Bittner F, Mendel RR, Kunze T, Clement B, and Havemeyer A (2014) Reduction of sulfamethoxazole hydroxylamine (SMX-HA) by the mitochondrial amidoxime reducing component (mARC). *Chem Res Toxicol* **27**:1687–1695.

Plitzko B, Havemeyer A, Kunze T, and Clement B (2015) The pivotal role of the mitochondrial amidoxime reducing component 2 in protecting human cells against apoptotic effects of the base analog *N*6-hydroxylaminopurine. *J Biol Chem* **290**:10126–10135.

Plitzko B, Ott G, Reichmann D, Henderson CJ, Wolf CR, Mendel R, Bittner F, Clement B, and Havemeyer A (2013) The involvement of mitochondrial amidoxime reducing components 1 and 2 and mitochondrial cytochrome b5 in *N*-reductive metabolism in human cells. *J Biol Chem* **288**:20228–20237.

Raedler LA (2016) Farydak (panobinostat): first HDAC inhibitor approved for patients with relapsed multiple myeloma. *Am Health Drug Benefits* **9** (Spec Feature):84–87.

Sparacino-Watkins CE, Tejero J, Sun B, Gauthier MC, Thomas J, Ragireddy V, Merchant BA, Wang J, Azarov I, Basu P, et al. (2014) Nitrite reductase and nitric-oxide synthase activity of the mitochondrial molybdopterins enzymes mARC1 and mARC2. *J Biol Chem* **289**:10345–10358.

Sugihara K, Kitamura S, and Tatsumi K (1983a) Evidence for reduction of hydroxamic acids to the corresponding amides by liver aldehyde oxidase. *Chem Pharm Biol (Tokyo)* **31**:3366–3369.

Sugihara K, Kitamura S, and Tatsumi K (1983b) Involvement of liver aldehyde oxidase in conversion of *N*-hydroxyurethane to urethane. *J Pharmacobiodyn* **6**:677–683.

Sugihara K and Tatsumi K (1986) Participation of liver aldehyde oxidase in reductive metabolism of hydroxamic acids to amides. *Arch Biochem Biophys* **247**:289–293.

Suzuki T, Matsuura A, Kouketsu A, Hisakawa S, Nakagawa H, and Miyata N (2005) Design and synthesis of non-hydroxamate histone deacetylase inhibitors: identification of a selective histone acetylating agent. *Bioorg Med Chem* **13**:4332–4342.

Vaughn JB, McGarvey PB, Lee MS, Garner CD, Wang CY, Linsmaier-Bednar EM, and King CM (1981) Activation of *N*-hydroxyphenacetin to mutagenic and nucleic acid-binding metabolites by acyltransfer, deacylation, and sulfate conjugation. *Cancer Res* **41**:3424–3429.

Verma RP (2012) Hydroxamic acids as matrix metalloproteinase inhibitors. *EXS* **103**:137–176.

Wagner JM, Hackanson B, Lübbert M, and Jung M (2010) Histone deacetylase (HDAC) inhibitors in recent clinical trials for cancer therapy. *Clin Epigenetics* **1**:117–136.

Wahl B, Reichmann D, Nicks D, Krompholz N, Havemeyer A, Clement B, Messerschmidt T, Rothkegel M, Biester H, Hille R, et al. (2010) Biochemical and spectroscopic characterization of the human mitochondrial amidoxime reducing components hmARC-1 and hmARC-2 suggests the existence of a new molybdenum enzyme family in eukaryotes. *J Biol Chem* **285**: 37847–37859.

Wang K and Guengerich FP (2013) Reduction of aromatic and heterocyclic aromatic *N*-hydroxylamines by human cytochrome P450 2S1. *Chem Res Toxicol* **26**:993–1004.

Whitby LG (1953) A new method for preparing flavin-adenine dinucleotide. *Biochem J* **54**: 437–442.

Wirth PJ, Dybing E, von Bahr C, and Thorgeirsson SS (1980) Mechanism of *N*-hydroxyacetylarylamines mutagenicity in the Salmonella test system: metabolic activation of *N*-hydroxyphenacetin by liver and kidney fractions from rat, mouse, hamster, and man. *Mol Pharmacol* **18**:117–127.

Wright SW and Corbett RL (1993) An efficient preparation of 2H-(5,4-b)Pyridoisothiazolone. *Org Prep Proced Int* **25**:247–249.

Zhang J and Zhong Q (2014) Histone deacetylase inhibitors and cell death. *Cell Mol Life Sci* **71**: 3885–3901.

Address correspondence to: Bernd Clement, Department of Pharmaceutical and Medicinal Chemistry, Pharmaceutical Institute, Christian-Albrechts-University of Kiel, Gutenbergstraße 76, 24118 Kiel, Germany. E-mail: bclement@pharmazie.uni-kiel.de

Supplemental Data

Article title: The Involvement of the Mitochondrial Amidoxime Reducing Component (mARC) in the Reductive Metabolism of Hydroxamic Acids

Authors: Carsten Ginsel, Birte Plitzko, Danilo Froriep, Diana A. Stofa, Manfred Jung, Christian Kubitza, Axel J. Scheidig, Antje Havemeyer, Bernd Clement

Journal title: Drug Metabolism and Disposition

DMD # 82453

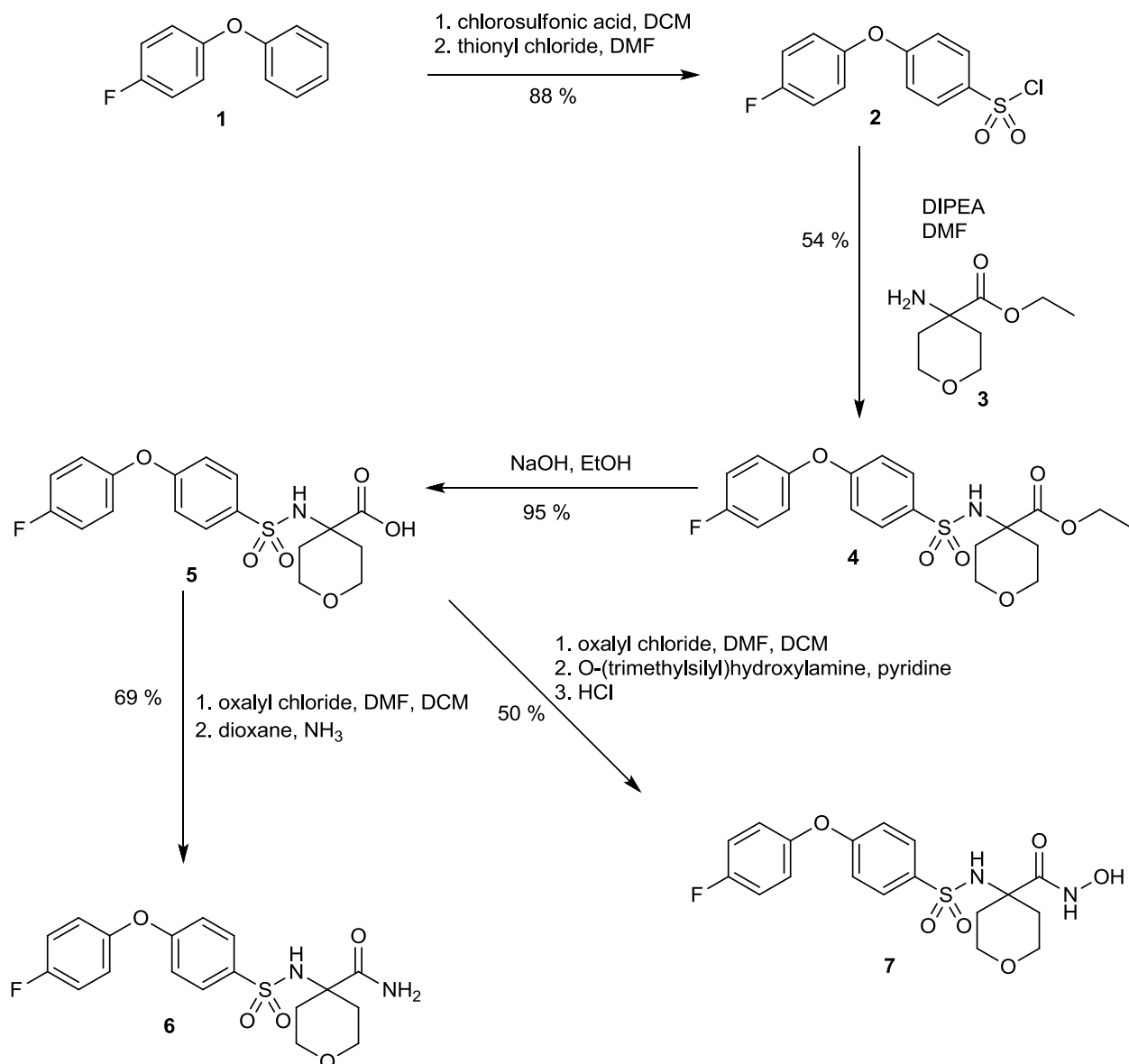
Legends to supplemental figures

Supplemental figure 1. Chemical synthesis for CP544439 (7) and related compounds

Supplemental figure 2. Influence of the DMSO concentration on the reduction of benzhydroxamic acid via mARC1. Marks are means \pm standard deviation of two biological determinations.

Supplemental figure 3. Influence of the DMSO concentration on the reduction of benzhydroxamic acid via mARC2. Marks are means \pm standard deviations of two biological determinations.

Supplemental figure 1



Synthesis of 4-(4-fluorophenoxy)benzene-sulfonyl chloride (2). **2** was prepared after the patent from Van Eck-Smit BLF, Pinas VA, and Windhorst AD, Radiolabelled MMP Selective Compounds, WO2009139634, 19.11.2009.

Synthesis of ethyl 4-((4-(4-fluorophenoxy)phenyl)-sulfonylamino)tetrahydropyran-4-carboxylate (4).

Ethyl 4-aminotetrahydro-pyran-4-carboxylate hydrochloride (**3**) was coupled with **2** to give **4** according to the patent from Reiter, Lawrence Alan, (4-arylsulfonylamino)-tetrahydropyran-4-carboxylic acid hydroxamides, US6087392, 21.10.1999.

Synthesis of 4-((4-(4-fluorophenoxy)phenyl)-sulfonylamino)tetrahydropyran-4-carboxylic acid (5). **4**

was treated with NaOH to give **5** according to the patent from Reiter, Lawrence Alan, (4-arylsulfonylamino)-tetrahydropyran-4-carboxylic acid hydroxamides, US6087392, 21.10.1999.

¹H-NMR (300 MHz, DMSO-d₆): δ 12.64 (s, 1H), 8.07 (s, 1H), 7.76 (d, *J* = 9.0 Hz, 2H), 7.33 – 7.27 (m, 2H), 7.21 – 7.16 (m, 2H), 7.08 (d, *J* = 9.0 Hz, 2H), 3.49 – 3.43 (m, 2H), 3.39 – 3.31 (m, 2H), 1.90 – 1.76 (m, 4H) ppm.

¹³C-NMR (75 MHz, DMSO-d₆): δ 174.0, 160.3, 158.9 (d, *J* = 240.8 Hz), 151.0 (d, *J* = 2.4 Hz), 137.0, 128.8, 122.0 (d, *J* = 8.7 Hz), 117.1 (d, *J* = 3.4 Hz), 116.8, 62.4, 58.1, 32.7 ppm.

LC-MS (ESI), *m/z* 396.0 [M+H]⁺.

Synthesis of 4-((4-(4-fluorophenoxy)phenyl)-sulfonylamino)tetrahydropyran-4-carboxamide (6). **6**

was synthesized as described by Crump CJ, Murrey HE, Ballard TE, Am Ende CW, Wu X, Gertsik N, Johnson DS, and Li Y-M (2016) Development of Sulfonamide Photoaffinity Inhibitors for Probing Cellular γ-Secretase. ACS Chem Neurosci 7:1166–1173.

¹H-NMR (300 MHz, DMSO-d₆): δ 7.79 – 7.76 (m, 3H), 7.33 – 7.27 (m, 2H), 7.21 – 7.17 (m, 2H), 7.07 (d, *J* = 9.0 Hz, 2H), 7.02 (s, 1H), 6.89 (s, 1H), 3.50 – 3.30 (m, 4H), 1.91 – 1.82 (m, 2H) ppm.

¹³C-NMR (75 MHz, DMSO-d₆): δ 174.2, 160.3, 158.9 (d, *J* = 240.9 Hz), 151.0 (d, *J* = 2.4 Hz), 136.7, 129.0, 122.0 (d, *J* = 8.7 Hz), 117.1, 116.8, 62.5, 58.8, 32.8 ppm.

LC-MS (ESI), *m/z* 395.1 [M+H]⁺.

Synthesis of 4-((4-(4-fluorophenoxy)phenyl)-sulfonylamino)tetrahydropyran-4-carbohydroxamic acid (7). For the synthesis of **7** the described method by Reiter, Lawrence Alan, (4-arylsulfonylamino)-tetrahydropyran-4-carboxylic acid hydroxamides, US6087392, 21.10.1999, was modified as followed: **5** (400 mg, 1.0 mmol) was dissolved in 4 ml DCM at room temperature. Oxalyl chloride (150 μ l, 1.7 mmol) and 4 drops DMF were added. The solution was stirred overnight. After cooling down the flask to 0 °C O-(trimethylsilyl)hydroxylamine (350 μ l, 2.3 mmol) and 300 μ l pyridine were added and the mixture was stirred for one hour at 0 °C and additional two hours at room temperature. The reaction was stopped by addition of 12 ml 2 N HCl and one hour additional stirring at room temperature. The formation of the product (brownish spot with FeCl₃) was controlled by TLC (cyclohexane/ethyl acetate 8:2). The organic phase was separated and the aqueous layer was extracted with 20 ml ethyl acetate three times. The combined organic layers were washed with water and brine. After drying with anhydrous NaSO₄ the solvent was evaporated to a volume of 15 ml and stored overnight at 4 °C. The resulting crystals were rinsed with cold cyclohexane/ ethyl acetate 1:1 and dried under high vacuum, yield 209 mg, 0.5 mmol (50 %).

¹H-NMR (300 MHz, DMSO-d₆): δ 10.37 (s, 1H), 8.69 (s, 1H), 7.80 – 7.74 (m, 3H), 7.33 – 7.24 (m, 2H), 7.22 – 7.15 (m, 2H), 7.07 (d, *J* = 8.9 Hz, 2H), 3.48 – 3.31 (m, 4H), 1.93 – 1.70 (m, 4H) ppm.

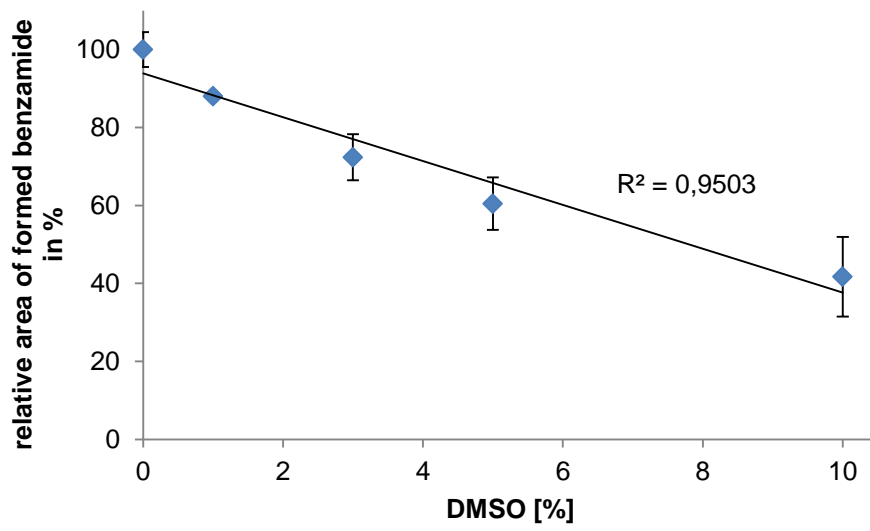
¹³C-NMR (75 MHz, DMSO-d₆): δ 169.0, 160.2, 158.9 (d, *J* = 240.9 Hz), 151.2 (d, *J* = 2.3 Hz), 137.0, 128.9, 121.8 (d, *J* = 8.6 Hz), 117.3, 116.9 (d, *J* = 23.5 Hz), 62.5, 58.0, 32.9 ppm.

LC-MS (ESI), *m/z* 411.1 [M+H]⁺.

Influence of DMSO addition to the incubation mixture:

For the studies of the DMSO-influence on the mARC1 and mARC2 activity, benzhydroxamic acid was chosen as the substrate and the quantification of benzamide as the outcome. All incubation mixture consisted of 3.75 μ g mARC, 37.5 pmol b5 and 3.75 pmol NADH b5 reductase in 20 mM MES buffer, pH 6.0. Substrate concentration was set to 3 mM and incubation time was 15 minutes at 37 °C in a shaking water bath. After 3 minutes of pre-incubation the reaction was started by addition of 1 mM NADH, resulting in a total volume of 150 μ l. The reaction was stopped with 150 μ l of cold methanol, followed by 5 minutes shaking and 5 minutes centrifugation at 9.500 g. The supernatants were analyzed via HPLC.

Supplemental figure 2



Supplemental figure 3

